

# Py-GC/MS of hydrochars produced from brewer's spent grains

M. P. Olszewski<sup>a\*</sup>, P. J. Arauzo<sup>a</sup>, M. Wądrzyk<sup>b,c</sup>, A. Kruse<sup>a</sup>

\* corresponding author: maciej.olszewski@uni-hohenheim.de

<sup>a</sup> Department of Conversion Technologies of Biobased Resources, Institute of Agricultural Engineering, University of Hohenheim, Garbenstrasse 9, 70599 Stuttgart, Germany

<sup>b</sup> Faculty of Energy and Fuels, AGH University of Science and Technology, al. Mickiewicza 30, 30-059 Krakow, Poland

<sup>c</sup> AGH Centre of Energy AGH University of Science and Technology, ul. Czarnowiejska 36, 30-054, Krakow, Poland

## Abstract

The aim of the study was to understand pyrolysis behavior and analyze the influence of hydrothermal carbonization (HTC) pretreatment on the volatile matter released during pyrolysis of hydrochars, produced from brewer's spent grains (BSG). The Py-GC/MS was used to analyze the pyrolysis products. The measurements were conducted for three hydrochars produced from BSG at different HTC conditions: (i) 180 °C, 4 h; (ii) 220 °C, 2 h; and (iii) 220 °C, 4 h, and the precursor BSG. The sample was pyrolyzed in the sequence at 300, 400, 500, and 600 °C with a heating rate of 500 °C min<sup>-1</sup> and residence time 15 s. Pyrolysis of BSG resulted in more phenolic compounds than hydrochars produced at mild conditions (HTC-180-4 and HTC-220-2). Pyrolysis of high-temperature hydrochar (HTC-220-4) showed the highest share of phenols due to the conversion of furan rings into benzene rings. Hydrochars (HTC-180-4 and HTC-220-2) produced more furans, and other cyclic oxygen compounds compared to the initial biomass. A significant amount of N-compounds was detected at low pyrolysis temperature for spent grains due to weakly bonded proteins into the biomass structure. However, hydrochars were characterized by fewer N-compounds compared to BSG because of the Maillard reaction occurred during hydrothermal pretreatment leading to N-heterocycles detected. Increased severity during the HTC resulted in a higher share of N-compounds found during Py-GC/MS.

## **Keywords**

Py-GC/MS; hydrochar; hydrothermal carbonization; pyrolysis; biomass; spent grain

## **1. Introduction**

Biomass is a potential source for overcoming the dependence of fossil resources for the production of energy, fuels, chemicals, and carbon materials. The transformations of the bio-based feedstock into several valuable products, *via* different thermochemical or biochemical technologies, are considered as the concept of the biorefinery. One of the most developed biomass thermochemical conversion technology used since ancient times is pyrolysis. The process consists of material decomposition under elevated temperature in the absence of oxygen. It results in the production of a solid residue called biochar, condensable organic matter called bio-oil, and non-condensable gases. However, pyrolysis is considered as the dry conversion technology. Therefore it is necessary to dry the feedstock before the process. The drying of biomass requires huge amounts of energy, due to this the possible feedstock for the conversion is limited to biomass with reasonable moisture content. The novel cascaded hydrothermal carbonization (HTC) followed by pyrolysis process can broaden the potential range of feedstock used in biorefinery as well as improve the overall energy efficiency of the process. The advantage of the hydrothermal carbonization process is the utilization of liquid water as a reaction medium; therefore, wet feedstock with water content up to 90 wt. % can be converted without previous drying. HTC operates at relatively mild temperatures (180-260 °C) and elevated pressure (above saturated steam pressure) to keep the water in liquid phase [1–7]. During the HTC process, the series of complex reaction occurs including hydrolysis, dehydration, decarboxylation, condensation, aromatization, and polymerization [2]. It results in the conversion of biopolymers contained into biomass; the hemicelluloses start to decompose at 180 °C, then celluloses begin degradation at 200 °C, lignin is converted at very low extend [2]. The final solid product called hydrochar is created by polymerization of solved intermediates in the liquid phase,

mainly 5-hydroxymethylfurfural (HMF) [2,3]. Additionally, liquid reaction medium eliminates/minimizes the heat transfer limitations compared to dry conversion technologies. The obtained hydrochar is hydrophobic, which results in more efficient mechanical dewatering as well as drying.

In this work brewer's spent grains (BSG) were selected for analysis as a potential feedstock for cascaded process due to high water content (after prior mechanical dewatering) 70-90 wt. % and huge worldwide production [8,9]. BSG is a waste lignocellulose stream generated by brewing industry. The properties of BSG depend on used barley and the brewing technology. Nevertheless, typical reported [10,11] composition consists of hemicellulose (21.8-40.2), cellulose (12.0-25.4), lignin (4.0-27.8), proteins (14.2-26.7), and lipids (3.9-13.3) in the wt. % dry basis.

For all those purposes fundamental pyrolysis study of volatile matter released during thermal decomposition of hydrochars and the initial brewer's spent grains is necessary to understand the pyrolysis mechanism, and as a consequence also the combustion behavior. Hydrochars were produced at different process conditions: i) 180 °C, 4h residence time; ii) 220 °C, 2h residence time; and iii) 220 °C, 4h residence time, to investigate the influence of HTC pretreatment for released pyrolysis vapors. All materials were pyrolyzed using Py-GC/MS to minimize the effect of the secondary reaction of the volatiles.

## 2. Methodology

### 2.1. Materials

The biomass for experiments was supplied by local brewery Hoepfner (Karlsruhe, Germany). The as-received brewer's spent grains (after prior mechanical dewatering) had a moisture content of ca. 78 wt. %. Part of the biomass was dried at 105 °C to constant mass and grind to achieve particle size below 200 µm for further analysis. The biomass was labeled as BSG and collected in a plastic zip bag. The rest of the biomass, to be used for further hydrothermal carbonization was stored in the freezer at -15 °C to avoid microbial attacks and keep moisture content as close as possible to original biomass.

HTC of BSG was carried out in a batch stainless steel autoclave of the volume of 250 mL, equipped with temperature and pressure sensor. Around 150 g of wet defrost BSG was filled into the reactor for each experiment. The reactor was placed in the GC oven (Hewlett Packard, GC 5890) and heated up to the desired temperature inside of the reactor in around 1 h. Then the reactor was kept at the desired temperature for set residence time. When the reaction time was reached, the reactor was quenched in cold water to the room temperature. Subsequently, the hydrochars were filtered using a paper filter (Qualitative filter paper 413, 5-13 µm, VWR European Cat, France) and a Büchner funnel. Afterwards, hydrochars were dried overnight at 105 °C and next ground to achieve particle size below 200 µm. The hydrochars were produced in three different process conditions: (i) 180 °C, 4 h residence time; (ii) 220 °C, 2 h; and (iii) 220 °C, 4 h. The hydrochars were respectively labeled as HTC-180-4, HTC-220-2, HTC-220-4 and stored in plastic zip bags.

## 2.2. Pyro-GC-MS

The decomposition studies of brewer's spent grains and hydrochars were carried out using pyrolysis and gas chromatography coupled to mass spectrometry (GC-MS) technique. Pyrolysis experiments were carried out using a Pyroprobe model 5200 (CDS Analytical), while the evolved during pyrolysis mixtures analyses were performed on GC-MS Agilent type GC 7890B equipped with an MS 5977A mass spectrometer. The pyrolysis tests were conducted at four different temperatures (300, 400, 500, and 600 °C) with a heating rate of 500 °C s<sup>-1</sup> and held time 15 s. Sample was placed inside a quartz tube, which subsequently was plugged from both sides with quartz wool and set at platinum filament. Before pyrolysis tests, the sample was purged from the air with an inert gas (Helium) for ca. 10 minutes. The pyrolysis was carried out in direct mode. The sample was pyrolyzed in sequence, starting at 300 °C, and following (the same sample) was heated to 400 °C, 500 °C, and 600 °C. Evolved during decomposition analytes were transferred for analysis to GC-MS *via* a transfer line. Pyrolysis interface and transfer line were kept at 300 °C. The Agilent HP-5MS capillary column of dimensions of 30 m × 0.25 mm × 0.25 μm was used. Helium of a grade of 6.0 was used as a carrier gas at a flow rate of 1.0 mL min<sup>-1</sup>. The GC injector temperature was kept at 300 °C. The analysis was performed at a split ratio of 75:1. The oven temperature was initially set to 40 °C with a hold time of 7 min, and then increased to 4 °C min<sup>-1</sup> until 250 °C. The ion source temperature was 230 °C, electron ionization was set at 70 eV, and spectra were scanned from 10–350 m/z. The obtained MS spectra were interpreted based on the reference MS library (chemical base G1034C). The threshold for the match factor calculated based on electronic library search routines was equal to 75%.

Additionally, the results were checked manually. Each analysis was repeated twice; the results were calculated as a mean value if the relative standard deviation was below 10%. The

contributions of detected compounds/group of compounds were computed relatively as a ratio of peak area of compounds to the summary peak area of all detected compounds. Peak area was determined in the total ion mode.

### 3. Results

#### 3.1. Ion pyrograms

To analyze the influence of hydrothermal carbonization on the pyrolysis of hydrochars the volatile matter composition was measured using Py-GC-MS. Pyrograms of spent grains and its hydrochars are shown in Fig. 1. Bio-based materials are characterized by large amounts of products due to the intense peaks related to the decomposition of biopolymers that built the structure of biomass [12].

#### 3.2. Pyro-GC-MS 500 °C

To show the difference caused by hydrothermal carbonization pretreatment, the decomposition products were divided into eight main groups: 1) phenols, 2) furans, 3) carboxylic acids and esters, 4) aliphatic oxygen compounds, 5) cyclic oxygen compounds, 6) N-compounds, 7) hydrocarbons (aromatic, cyclic, aliphatic), 8) complex high molecular weight compounds ( $M_w > 300 \text{ g mol}^{-1}$ ). The relative shares [%] of the different groups of pyrolysis products of brewer's spent grains and hydrochars are shown in Fig. 2. The main compounds detected during Py-GC/MS analysis are summarized in Table 1. The relative content of phenols for BSG was 26.8% and 9.7%, 11.4%, 32.7% for HTC-180-4, HTC-220-2, and HTC-220-4, respectively. The next group of identified compounds was furans. Percentage share of furans for the feedstock was 8.9% and 19.6%, 20.7%, 0% for HTC-180-4, HTC-220-2, and HTC-220-4, respectively. The share of furans increased for hydrochars compared to biomass except for HTC-220-4, where the furans were not identified. The relative share of carboxylic acids and esters for BSG was 17.8% and 30.6%, 19.9%, 22.9% for HTC-180-4, HTC-220-4, and HTC-220-4, respectively. The share of other aliphatic oxygen compounds was 4.3%, 5.8%, 9.6%, 0.7%; while, the content of other cyclic oxygen compounds was 9.7%, 13.3%, 13.6%, 25.3% for BSG, HTC-180-4, HTC-220-2, HTC-220-4, respectively. The highest relative share of N-compounds in pyrolysis vapors was found for brewer's spent grains

(28.2%). The share of N-compounds for hydrochars was 4.6%, 6.0%, 11.9% for HTC-180-4, HTC-220-2, and HTC-220-4, respectively. Additionally, due to the complex structure of the analyzed materials, hydrocarbons, as well as complex compounds, were secreted.

### 3.3. Compounds released as a function of pyrolysis temperature

The distribution of chemical groups as a function of the pyrolysis temperature for investigated materials is shown in Fig. 3. The lowest shares of phenols were observed for HTC-180-4 and HTC-220-2 which did not show a clear trend. At the initial pyrolysis temperature, the highest yield of phenols was achieved for HTC-220-4 which increased at 400 °C reaching the maximum. Further increasing of the pyrolysis temperature reduced the phenolic compounds share in the decomposition products. The relative content of phenols released during pyrolysis of initial biomass were lower compared to HTC-220-4, and the maximum share was achieved at 500 °C. The release of furans at 300 °C was the highest for brewer's spent grains and close to zero for HTC-180-4, and HTC-220-2. The shares raised rapidly for hydrochars and were topped at 400 °C; then the release was depleted at 600 °C. Furans were not detected for HTC-220-4. Carboxylic acids and esters found in pyrolysis products showed a higher yield for hydrochars at 300 °C compared to biomass. Increased pyrolysis temperature (400 °C) lead to a higher yield for HTC-180-4, then the share reached a minimum at 500 °C. The highest investigated temperature resulted in a maximum yield of carboxylic acids and esters for this material. On the other hand, the share of other hydrochars dropped sharply with increasing pyrolysis temperature. The share for biomass showed mild fall during increasing severity of the pyrolysis. The share of other aliphatic oxygen compounds at 300 °C showed the highest value for HTC-180-4; however, the temperature rise caused a reduction in the relative amount for this material. HTC-220-4 produced the lowest yield at every stage of the pyrolysis, showing a growth trend when the temperature of the analysis

increased. Biomass and HTC-220-2 showed minimum yield at 300 °C and then sharply increased at 400 °C, further increasing of the pyrolysis temperature result in a lower share of this group in pyrolysis vapors. At 600 °C relative yield for biomass continued dropping, while HTC-220-2 increased. Other cyclic oxygen compounds were released with the highest share for HTC-180-4 at the lowest pyrolysis temperature (300 °C); however, increasing the temperature of pyrolysis caused a decrease in the share. HTC-220-4 also showed a high share of other cyclic oxygen compounds at low pyrolysis temperature, but the share grew with increasing the pyrolysis temperature and reached a maximum at 500 °C. For origin biomass, the share was the lowest at the initial stage of the pyrolysis and raised at higher pyrolysis temperatures. N-compounds were detected with the highest yield for precursor at 300 °C, and then fell sharply at higher analysis temperatures. Hydrochars showed a similar trend, and the share slightly decreased at 400 °C, afterward gently rose at higher temperatures. The amount of released N-compounds was higher for hydrochars produced with higher severity. Hydrocarbons were detected for all materials at early pyrolysis stage at relatively low concentrations. Higher pyrolysis temperature led to a sharp yield increase for HTC-220-2 and HTC-180-4; however, the share for BSG and HTC-220-4 rose slightly. Complex compounds reached the maximum share for HTC-180-4 at lowest pyrolysis temperature, then dropped at 400 °C and rose again at higher temperatures. For other materials the share of complex compounds was meager; nevertheless, the trend showed decreased shares for higher pyrolysis temperatures.

#### 4. Discussion

It has to be stated that the composition of compounds measured after Py-GC-MS are more similar than it can be assumed because of the differences in the Arrhenius parameters studied previously. The reason is that biomass is pyrolyzed in Py-GC/MS. Therefore, pyrolysis products are formed and immediately analyzed. On the other hand, this is compared with carbonization products volatilized or pyrolysis. The products measured in Py-GC/MS must be similar. To see a difference as a consequence of the changed material structure, the details are important.

Hydrothermal carbonization process converts biopolymers contained into biomass to hydrochar. However, the degradation products showed some similarities - common detected compounds during Py-GC/MS (Fig. 1, Table 1). It may result from characteristic composition and structure of initial biomass (specific cross-linking and interconnection of biomass species, for example with lignin) which was not converted during the HTC process. Nevertheless, during pyrolysis, high-temperature conversion can break the structure into some characteristic compounds. This phenomenon is very often used in analytical pyrolysis, where Py-GC/MS is used for determination of the origin of materials by identification of marker compounds, for example, wood species [13,14]. Additionally, the decomposition of polymerized hydrochar and initial feedstock may release similar compounds during pyrolysis due to thermal destruction of the chemical bonds.

On the other hand, Py-GC/MS analysis showed that during pyrolysis of hydrochars new compounds were found compared to pyrolysis of the initial biomass (Fig. 1). It might result from the structural change of the initial biomass caused by HTC pretreatment.

## **Phenols**

Phenols are natural ingredients of BSG [10]. Partly they are solved during HTC, which leads to the lower amount for low-temperature hydrochar (Fig. 2). Due to the conversion of furan-rings to benzene-rings at the higher temperature, the phenol content is higher for high-temperature hydrochars [6,15]. The lower share of phenols from hydrochars produced at milder conditions (HTC-180-4 and HTC-220-2) compare to biomass may be due to the conversion of carbohydrates during the HTC process. The longer residence time for the last hydrochar caused further cellulose decomposition and consequently higher carbonization degree. This may result in increased production of phenolic compounds. Guaiacol (2-methoxyphenol, Table 1) appearing in the pyrolysis products of raw biomass and hydrochar is the main product of pyrolysis of lignin [16]. The 4-ethenyl-2-methoxyphenol is commonly found in beer made from wheat. It is created from the ferulic acid by thermal or enzymatic decarboxylation, and it is responsible for the characteristic flavor of the 'white beer' [17]. This compound was also found in the Py-GC-MS analysis of aroma produced from buckwheat [18]. The phenols may also be formed by thermal decomposition of side parts of some amino acids which built proteins contained in the feedstock [19] as well as hydrothermal treatment of cellulose and carbohydrates but in rather higher temperatures [20,21].

## **Furans**

Furfural and 5-hydroxymethylfurfural (HMF) are products from the elimination of water from sugars and higher carbohydrates. They are always formed if biomass is pyrolyzed [7,22,23]. Additionally, they are the main structural part of the hydrochars produced in mild conditions [7]; therefore, the content is higher after Py-GC-MS for hydrochars (Fig. 2). HMF is thermally labile and forms via decarbonylation 2-furanmethanol or furfural (Table 1). Furfural and the consecutive

product of HMF 2-furanmethanol are only found in the case of BSG (Table 1) because only the biomass has high amounts of carbohydrates. Fig. 3 shows that the furans are also formed at higher pyrolysis temperatures in the case of BSG. This leads to the assumption that they are formed from cellulose degradation. Cellulose is rather a thermal stable because H-bonds stabilize it.

During hydrothermal carbonization, HMF is formed as well. By its polymerization, likely aldol condensation, the structure the hydrochar is formed [24,25]. In Fig. 3 the volatilization of the furans is the highest at 400 and 500 °C for the HTC-180-4 and HTC-220-2. What is visible here is a kind of de-polymerization, but not by the reverse reaction of the formation. The retro-aldol condensation would need the water as a reactant, which is not present at Py-GC conditions. Instead, a free radical splitting occurs, which fits the temperature range of 400-500 °C. The free radical reaction, induced by the high temperature, leads to a C-C split. Therefore, not the original HMF and its consecutive products furfural and furanmethanol but methyl-furans are formed. The methyl-groups are part of the neighboring furan-ring in the hydrochar structure. With increasing severity, here the hydrochar HTC-220-4, a transformation to aromatic structures and stronger cross-linking occurs [26]. This means furanic structure parts could not be formed anymore, because they do not exist anymore or they are too strongly inter-connected leading to a complete fragmentation during pyrolysis.

The furfural released during pyrolysis of BSG is mainly formed through direct degradation of oligosaccharides [27]. The detection of 2, 5-dimethylfuran is related with the decomposition of cellulose [12]; however, in the case of hydrochars, it may also be degradation of the structure created by the polymerization of 5-HMF. The lack of furans for the last hydrochar may be related with the high share of other cyclic oxygen compounds that could be promoted during the decomposition. The higher cross-linking of high-temperature hydrochar may lead to a splitting of

the furanic rings, which are there in a lower relative amount. Zhang et al. [28] also detected 2-ethyl furan during Py-GC-MS of hydrochars produced from municipal sewage sludge.

### **Carboxylic acids and esters**

Acetic acid was only detected for vapors released from biomass; it is mainly produced by thermal degradation of hemicellulose [29]. The lack of acetic acid in case of hydrochars pyrolysis confirmed that hemicellulose was converted during the hydrothermal carbonization process. Palmitic acid, linoleic acid, oleic acid, and linolelaidic acid are fatty acids which occur in the structure of plants [30]. Mild HTC conditions leave the fatty acids unchanged; they can be extracted after HTC [31]. Therefore, n-hexadecanoic acid, linoleic acid, other fatty acids, and their derivatives can be identified in Py-GC/MS (Table 1). Linoleic acid as an unsaturated compound is supposed to be less stable as, e.g., hexadecanoic acid, which might lead to a decrease at higher temperatures (Table 1). The product of an oxidative cleavage of an unsaturated fatty acid could be shorter aldehyde like hecanal or ocatanal. Octanal is found after Py-GC (Table 1). The glycidil oleate (Table 1) indicates that the fatty acids are formed via hydrolysis of fats and oils during HTC.

### **Other oxygen compounds**

The relative yield of aliphatic oxygen compounds increased for HTC-180-4 and HTC-220-2 compared to the initial material; however, the concentration decreased for HTC-220-4. The main detected compound in this group: 3-methylbutanal (Table 1) also known as iso-Valeraldehyde is a chemical compound commonly present in chemical profile of alcoholic drinks (beer, sake, and distillates) [32,33]. The preference of the formation of aromatic or other cyclic compounds also explains the decrease of aliphatic and increase of aromatic oxygen compounds for the high-temperature hydrochar with the complete conversion (Fig. 2). It may result from the most carbonized

structure *via* polymerization of 5-HMF during hydrothermal carbonization, which may favor degradation to the cyclic oxygen compound.

Cyclopentanone, especially hydroxymethyl-cyclopentanone is formed by rearrangement of HMF [34]. Therefore, it is mainly found in Py-GC of biomass, because of the same reason like for furfural (see above).

### **N-compounds**

The high content of nitrogen-containing compounds was detected during Py-GC/MS analysis; it is related to the high protein content of origin biomass [10,11]. During the hydrothermal treatment of BSG, the proteins are hydrolyzed to amino acids. These amino acids can further react by hydrolysis and elimination of ammonia and formation of carboxylic acids or by decarboxylation and the formation of an amine. Amino acids and ammonia are solved in the water, leading to lower nitrogen content in the hydrochar compared to the original feedstock [35]. As the yield of hydrochar decrease with the temperature of the HTC process, the relative yield of N-compounds detected during Py-GC/MS analysis increase (Fig. 2). In BSG the proteins are not strongly bonded and therefore are volatilized at a relative low pyrolysis temperature (Fig. 3). During pyrolysis, the proteins are chemically converted, and could not be identified anymore. Important is that only in the case of the original biomass an oxazolidine was identified in relevant amounts (Table 1). It can be regarded as the direct consecutive product of amino acids.

During HTC, the Maillard reaction happens, which means that N-containing heterocyclic compounds are formed [35]. This happens to the minor part of amino acids formed from hydrolysis. This is better investigated for hydrothermal liquefaction [36,37]. These heterocyclic compounds are integrated into the polymeric structure of the hydrochar [38]. Therefore, these compounds are

volatilized at rather high temperatures (Fig. 3) compared to the BSG results. At these temperatures the structures are completely split, leading to diverse N-containing compounds (Table 1).

### **Hydrocarbons**

The decarboxylation of fatty acids leads to saturated hydrocarbons, the rearrangement of furfural-rings to phenols and other aromatic ring compounds. In each case hydrocarbons, if they are not in the original biomass, are late consecutive products and the exact reaction pathway is difficult to identify. In the case of Toluene, the less severe HTC conditions lead to higher amounts in Py-GC as the original biomass or HTC-220-4. As the aromatic can be formed by transformation of furanic rings, it is clear that toluene amount is lower in the case of BSG. The lower amount for HTC-220-4 is more difficult to explain. An assumption could be that the higher solubility of less-polar compounds [3] and the long reaction time leads to an extraction of possible pre-cursors from the hydrochar. In this case, clear hints are missing yet.

## 5. Conclusion

The study aimed to analyze the pyrolysis behavior of hydrochars produced from brewer's spent grains. The hydrothermal carbonization was carried out in a batch stainless steel autoclaves. Three hydrochars were produced at different process conditions to investigate the influence of the HTC pretreatment on the pyrolysis mechanism. The volatiles released during pyrolysis were analyzed by Py-GC/MS. The measurements were carried out in sequence at 300, 400, 500, and 600 °C with a heating rate of 500 °C min<sup>-1</sup> and residence time 15 s. The composition of pyrolysis gases for brewer's spent grains and hydrochars showed some similarities which can result from the origin of the biomass; however, many different compounds were also detected. BSG released more phenolic derivative compounds than hydrochars produced with lower severity, where phenols were partially solved during the HTC. However, the phenols content was higher for high-temperature hydrochar due to the conversion of furan-rings to benzene-rings at higher temperatures. Hydrochars produced more furans as well as other cyclic oxygen compounds than biomass because they are the main structural part of the hydrochar. In the case of biomass, furans are created from degradations of sugars or higher carbohydrates. Acetic acid the main product of hemicellulose pyrolysis was detected only for initial biomass; it confirms that the hemicellulose was converted during the HTC pretreatment. Mild HTC conditions leave the fatty acids unchanged. A significant amount of N-compounds was released at relatively low temperature during pyrolysis of raw BSG due to weakly bonded proteins. Fewer N-compounds was detected for pyrolysis of hydrochars due to Maillard reaction occurred during HTC pretreatment. N-compounds in hydrochar are stable due to their aromatic structure. The relative share in Py-GC/MS products showed the slightly higher yield with increasing the severity of the HTC process. It is related to the lower hydrochar yield and a higher concentration of N-compounds. The differences found during Py-GC/MS may confirm the different structure of the hydrochars compared to the precursor caused by the hydrothermal treatment. The pyrolyzed hydrochars may also show various material properties, e.g., surface area, electrical conductivity, etc., which can draw the attention of other scientists.

## Acknowledgments

This project has received funding from the European Union's Horizon 2020 research and innovation programme under the Marie Skłodowska-Curie grant agreement No 721991. The Py/GC-MS research was carried out using the infrastructure of the AGH Centre of Energy.

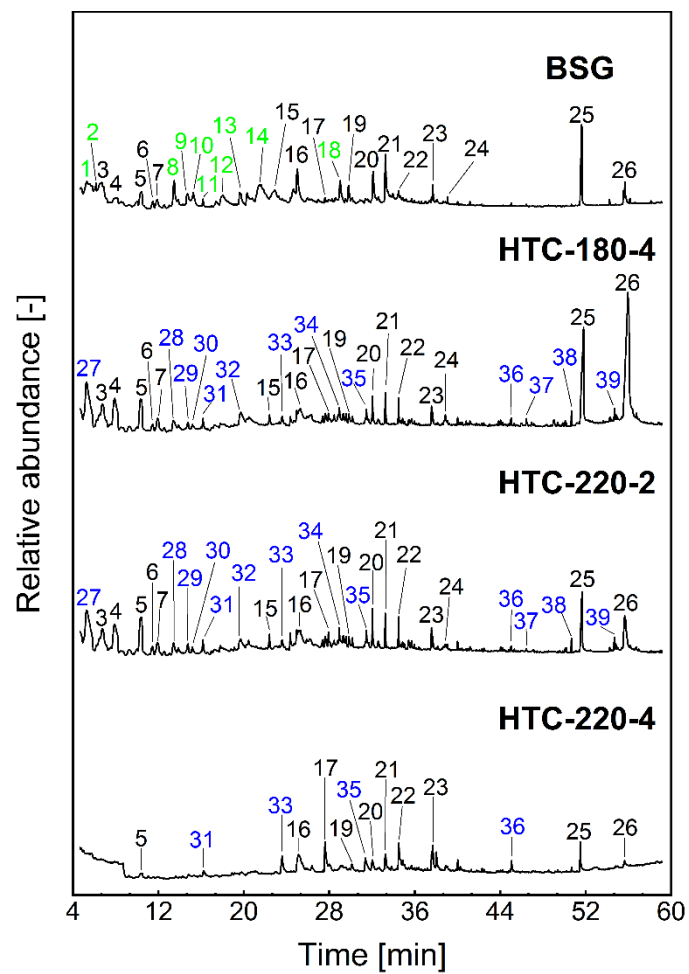


Fig. 1. Ion pyrograms for brewer's spent grains and hydrochars, Py-GC/MS 300-400 °C (black – common for all materials, green – characteristic for the precursor, blue – characteristic for hydrochars).

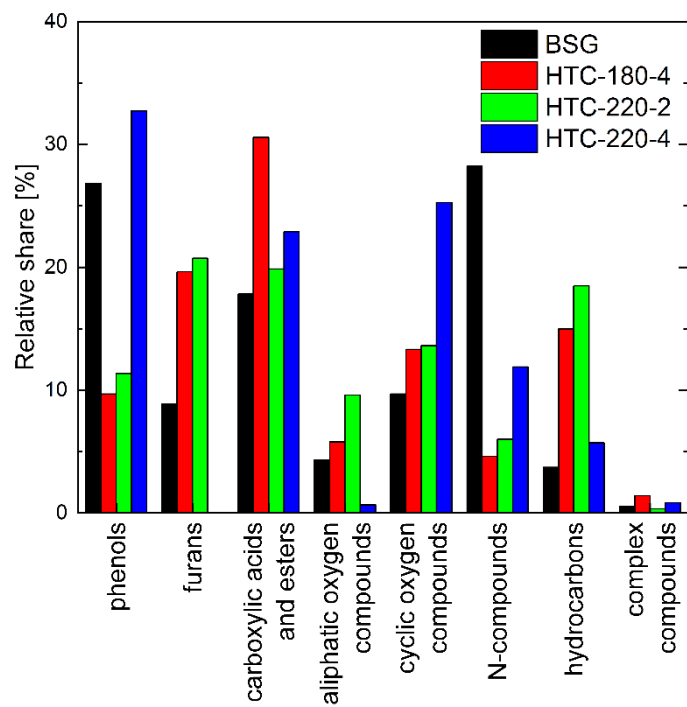


Fig. 2. The relative share of different chemical groups of compounds released during Py-GC-MS at 500 °C.

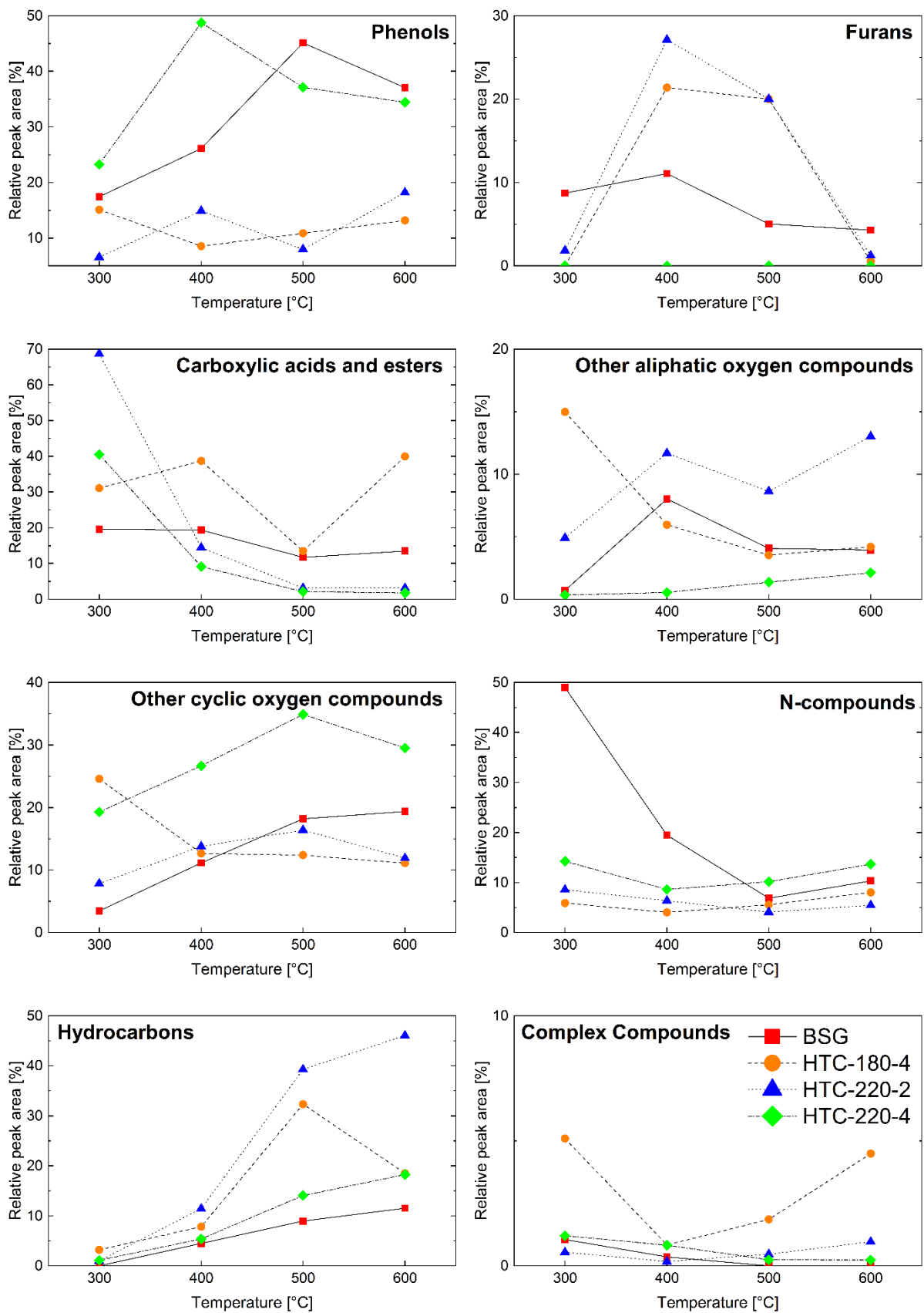


Fig. 3. Peak area changes for chemical groups of compounds as a function of pyrolysis temperature.

Table 1

Summary of selected compounds released during Py-GC-MS at 500 °C assignment to their chemical groups.

Peak No	Chemical Group	Compound	Relative share [%]				
			BSG	HTC-180-4	HTC-220-2	HTC-220-4	
3	aliphatic oxygen comp.	3-methyl-butanal	2.87	4.58	6.38	-	
6		octanal	-	1.20	1.58	0.29	
		9-heptadecene-4,6-diyn-3-ol	-	-	0.42	0.38	
13		decanal	2.50	-	-	-	
1	other cyclic oxygen compounds	1,2-diol- cis- 3-cyclopentene	1.25	-	-	2.15	
7		trans-1,2-cyclopentane diol	1.84	-	3.28	1.53	
16		2-hydroxy-3-methyl-2-cyclopenten-1-one	1.92	0.74	0.53	-	
		1-cyclohexene-1-methanol	-	1.07	1.20	-	
28		1,4-cyclohexanedimethanol	-	0.90	1.27	-	
32		4,5-dimethylperhydro-2-(1,1-dimethylethyl)-1,3-benzodioxin-4-one	-	1.98	1.16	1.63	
33		1-methyl-4-(1-methylethenyl)-trans-2-cyclohexen-1-ol	-	0.68	0.55	6.01	
17		octahydro-2,4-dimethanopentalene-3,6-diol	0.64	0.88	0.96	7.17	
		3,4,7,8,9,10-hexahydro-4-hydroxy-10-methyl-2h-oxecin-2-one	0.03	0.50	0.17	0.18	
		tetracyclo-dodec-3-en-11-ol	0.07	0.30	0.32	0.52	
		1,2,3,4,4a,5,6,7-octahydro-4a-methyl-2-naphthol	-	0.67	1.04	1.17	
		2-(2-methyl-propenyl)-cyclohexanone	-	0.21	0.20	0.17	
		3-hydroxy- $\alpha$ -ionene	-	0.23	0.16	0.54	
		1,2,3,4-bis(epoxy)-2,6,6-trimethyl-1-pent-2-en-4-one-2-yl cyclohexane	-	0.42	0.21	0.53	
2		carboxylic acids and esters	acetic acid	0.66	-	-	0.13
11			2-phenylethyl hexanoic acid ester	0.94	-	-	-
24	heranyl 3-methylbutanoate		0.55	0.21	0.31	0.36	
25	n-hexadecanoic acid		9.10	10.60	10.64	16.33	
26	linoleic acid		0.92	13.51	3.83	1.94	
37	12-acetoxy-2-methoxy-6,10-dimethyl-dodeca-2E, 6Z, 10Z-trienoic acid, methyl ester		-	0.33	0.33	0.28	

38		13-methyl-pentadecanoic acid, methyl ester	-	1.00	0.60	0.56	
39		8,11-octadecadienoic acid, methyl ester	-	0.52	0.45	0.17	
		glycidyl oleate	-	0.25	0.25	0.11	
		cis-9-octadecenoic acid	-	3.02	2.21	2.26	
		3-methylphenol	2.51	0.24	0.96	1.29	
17		2-methoxyphenol	4.94	0.36	2.84	9.77	
18		2-methoxy-4-methylphenol	2.37	-	-	-	
20		4-ethyl-2-methoxyphenol	3.02	1.97	2.02	3.87	
21	phenol and derivatives	2-methyl-5-(1-methylethyl) phenol	9.86	1.70	1.35	2.35	
		4-methoxy-3-(methoxymethyl)-phenol	0.14	0.66	0.75	1.91	
23		2-methoxy-5-(1-propenyl)-(E)-phenol	1.11	0.57	0.46	3.04	
35		4-methoxybenzene-1,2-diol	-	1.51	1.05	2.86	
22		2,4-dimethoxyphenol	0.95	1.23	0.93	3.99	
36		2,6-dimethoxy-4-(2-propenyl) phenol	-	0.59	0.31	1.81	
34		2,5-dimethyl-1,4-benzenediol	-	0.75	0.56	1.18	
4		furans	2,5-dimethyl-furan	2.74	6.39	6.59	-
8			furfural	4.18	-	-	-
9			2-furanmethanol	1.96	-	-	-
27	2-methyl-furan		-	13.23	14.14	-	
12	N-compounds	2-amino-5-(2-piperidin-1-ylethyl)-[1,3,4]thiadiazol	2.38	-	-	-	
15		2,2-diethyl-3-methyl-oxazolidine	24.33	-	-	-	
		4-(2,5-dihydro-3-methoxyphenyl)butylamine	0.17	0.60	0.54	0.17	
19		4,4a,5,6-tetrahydro-2(3H)-naphthalenone	1.92	0.46	0.54	0.13	
		2-(4-nitrophenyl)acetamide	0.16	0.41	0.30	0.00	
		N-methyl-N-[4-(3-hydroxypyrrolidinyl)-2-butynyl]-acetamide	0.12	1.20	0.38	2.19	

		2-methyl-5-(1-methylethyl)-7-azabicyclo[4.1.0]heptane	-	0.92	0.45	-
		2-(1-methyl-2-nitroethyl)cyclohexanone	0.18	0.26	0.34	-
		N-methyl-N-4-[1-(pyrrolidinyl)-2-butynyl]-formamide	-	0.19	0.31	1.37
		N-methyl-N-[4-(3-hydroxypyrrolidinyl)-2-butynyl]-acetamide	-	1.09	0.33	0.75
		2,3,5-trimethoxyamphetamine	-	0.25	0.26	1.10
		octahydro-2,4a,8,8-tetramethyl-, oxime cyclopropa[d]naphthalen-3-one	-	-	0.45	0.64
		2-(2-isopropenyl-5-methyl-cyclopentyl)-acetamide	-	-	-	2.93
5	hydro-carbons (Mw>300 g.mol <sup>-1</sup> )	toluene	3.71	11.02	12.53	3.12
29		1,3-dimethylbenzene	-	1.19	1.79	0.86
30		1,4-dimethylbenzene	-	0.62	0.76	-
31		styrene	-	1.58	2.25	1.72
		nonane	-	0.25	0.47	-
		trans 9-octadecenoic acid (2-phenyl-1,3-dioxolan-4-yl) methyl ester	-	0.29	0.05	0.27

## Literature

- [1] J. Poerschmann, B. Weiner, H. Wedwitschka, I. Baskyr, R. Koehler, F.D. Kopinke, Characterization of biocoals and dissolved organic matter phases obtained upon hydrothermal carbonization of brewer's spent grain, *Bioresour. Technol.* 164 (2014) 162–169. doi:10.1016/j.biortech.2014.04.052.
- [2] A. Funke, F. Ziegler, Hydrothermal carbonization of biomass: A summary and discussion of chemical mechanisms for process engineering, *Biofuels, Bioprod. Biorefining.* 4 (2010) 160–177. doi:10.1002/bbb.198.
- [3] A. Kruse, N. Dahmen, Water - A magic solvent for biomass conversion, *J. Supercrit. Fluids.* 96 (2015) 36–45. doi:10.1016/j.supflu.2014.09.038.
- [4] X. Zhu, Y. Liu, F. Qian, S. Zhang, J. Chen, Investigation on the Physical and Chemical Properties of Hydrochar and Its Derived Pyrolysis Char for Their Potential Application: Influence of Hydrothermal Carbonization Conditions, *Energy and Fuels.* 29 (2015) 5222–5230. doi:10.1021/acs.energyfuels.5b00512.
- [5] Y. Shen, S. Yu, S. Ge, X. Chen, X. Ge, M. Chen, Hydrothermal carbonization of medical wastes and lignocellulosic biomass for solid fuel production from lab-scale to pilot-scale, *Energy.* 118 (2017) 312–323. doi:10.1016/j.energy.2016.12.047.
- [6] M.-M. Titirici, R.J. White, C. Falco, M. Sevilla, Black perspectives for a green future: hydrothermal carbons for environment protection and energy storage, *Energy Environ. Sci.* 5 (2012) 6796. doi:10.1039/c2ee21166a.
- [7] J.A. Libra, K.S. Ro, C. Kammann, A. Funke, N.D. Berge, Y. Neubauer, M.-M. Titirici, C. Fühner, O. Bens, J. Kern, K.-H. Emmerich, Hydrothermal carbonization of biomass residuals: a comparative review of the chemistry, processes and applications of wet and dry pyrolysis, *Biofuels.* 2 (2011) 71–106. doi:10.4155/bfs.10.81.
- [8] Statista, Beer Production Worldwide From 1998 to 2016, *Stat. Portal.* (2017). <https://www.statista.com/statistics/270275/worldwide-beer-production/> (accessed May 8, 2018).
- [9] Barth-Haas Group, *The Barth Report*, (2015) 32. doi:53093-1505-1002.
- [10] A.L. McCarthy, Y.C. O'Callaghan, C.O. Piggott, R.J. FitzGerald, N.M. O'Brien, Brewers' spent grain; Bioactivity of phenolic component, its role in animal nutrition and potential for incorporation in functional foods: A review, *Proc. Nutr. Soc.* 72 (2013) 117–125. doi:10.1017/S0029665112002820.
- [11] P. Niemi, T. Tamminen, A. Smeds, K. Viljanen, T. Ohra-Aho, U. Holopainen-Mantila, C.B. Faulds, K. Poutanen, J. Buchert, Characterization of lipids and lignans in brewer's spent grain and its enzymatically extracted fraction, *J. Agric. Food Chem.* 60 (2012) 9910–9917. doi:10.1021/jf302684x.
- [12] R. Conti, A.G. Rombolà, A. Modelli, C. Torri, D. Fabbri, Evaluation of the thermal and environmental stability of switchgrass biochars by Py-GC-MS, *J. Anal. Appl. Pyrolysis.* 110 (2014) 239–247. doi:10.1016/j.jaap.2014.09.010.
- [13] M. Traoré, J. Kaal, A. Martínez Cortizas, Potential of pyrolysis-GC-MS molecular fingerprint as a proxy of Modern Age Iberian shipwreck wood preservation, *J. Anal. Appl. Pyrolysis.* 126 (2017) 1–13. doi:https://doi.org/10.1016/j.jaap.2017.07.003.

- [14] C. Schwarzingler, M. List, Identification of marker compounds in pyrolysis–GC/MS of various acetylated wood types, *J. Anal. Appl. Pyrolysis*. 87 (2010) 144–153. doi:<https://doi.org/10.1016/j.jaap.2009.11.001>.
- [15] C. Falco, F. Perez Caballero, F. Babonneau, C. Gervais, G. Laurent, M.M. Titirici, N. Baccile, Hydrothermal carbon from biomass: Structural differences between hydrothermal and pyrolyzed carbons via <sup>13</sup>C solid state NMR, *Langmuir*. 27 (2011) 14460–14471. doi:10.1021/la202361p.
- [16] T. He, Y. Zhang, Y. Zhu, W. Wen, Y. Pan, J. Wu, J. Wu, Pyrolysis Mechanism Study of Lignin Model Compounds by Synchrotron Vacuum Ultraviolet Photoionization Mass Spectrometry, *Energy & Fuels*. 30 (2016) 2204–2208. doi:10.1021/acs.energyfuels.5b02635.
- [17] L.C. Verhagen, 3.22 - Beer Flavor, in: H.-W. (Ben) Liu, L.B.T.-C.N.P.I.I. Mander (Eds.), Elsevier, Oxford, 2010: pp. 967–997. doi:<https://doi.org/10.1016/B978-008045382-8.00087-3>.
- [18] D. Janeš, D. Kantar, S. Kreft, H. Prosen, Identification of buckwheat (*Fagopyrum esculentum* Moench) aroma compounds with GC–MS, *Food Chem.* 112 (2009) 120–124. doi:<https://doi.org/10.1016/j.foodchem.2008.05.048>.
- [19] G. Chiavari, G.C. Galletti, Pyrolysis—gas chromatography/mass spectrometry of amino acids, *J. Anal. Appl. Pyrolysis*. 24 (1992) 123–137. doi:[https://doi.org/10.1016/0165-2370\(92\)85024-F](https://doi.org/10.1016/0165-2370(92)85024-F).
- [20] P.T. Williams, J. Onwudili, Composition of Products from the Supercritical Water Gasification of Glucose: A Model Biomass Compound, *Ind. Eng. Chem. Res.* 44 (2005) 8739–8749. doi:10.1021/ie050733y.
- [21] A. Sinaž, A. Kruse, V. Schwarzkopf, Key Compounds of the Hydrolysis of Glucose in Supercritical Water in the Presence of K<sub>2</sub>CO<sub>3</sub>, *Ind. Eng. Chem. Res.* 42 (2003) 3516–3521. doi:10.1021/ie030079r.
- [22] X.-N. Ye, Q. Lu, X. Wang, T.-P. Wang, H.-Q. Guo, M.-S. Cui, C.-Q. Dong, Y.-P. Yang, Fast Pyrolysis of Corn Stalks at Different Growth Stages to Selectively Produce 4-Vinyl Phenol and 5-Hydroxymethyl Furfural, *Waste and Biomass Valorization*. (2018). doi:10.1007/s12649-018-0259-0.
- [23] D. Shen, The Overview of Thermal Decomposition of Cellulose in Lignocellulosic Biomass, in: R. Xiao (Ed.), IntechOpen, Rijeka, 2013: p. Ch. 9. doi:10.5772/51883.
- [24] C. Falco, N. Baccile, M.-M. Titirici, Morphological and structural differences between glucose, cellulose and lignocellulosic biomass derived hydrothermal carbons, *Green Chem.* 13 (2011) 3273–3281. doi:10.1039/C1GC15742F.
- [25] A. Kruse, A. Funke, M.-M. Titirici, Hydrothermal conversion of biomass to fuels and energetic materials, *Curr. Opin. Chem. Biol.* 17 (2013) 515–521. doi:<https://doi.org/10.1016/j.cbpa.2013.05.004>.
- [26] A. Kruse, T. Zevaco, Properties of Hydrochar as Function of Feedstock, Reaction Conditions and Post-Treatment, *Energies*. 11 (2018) 674. doi:10.3390/en11030674.
- [27] X. Chen, H. Yang, Y. Chen, W. Chen, T. Lei, W. Zhang, H. Chen, Catalytic fast pyrolysis of biomass to produce furfural using heterogeneous catalysts, *J. Anal. Appl. Pyrolysis*. 127 (2017) 292–298. doi:<https://doi.org/10.1016/j.jaap.2017.07.022>.
- [28] J. ZHANG, Q. LIN, X. ZHAO, The Hydrochar Characters of Municipal Sewage Sludge Under Different Hydrothermal Temperatures and Durations, *J. Integr. Agric.* 13 (2014) 471–482.

doi:[https://doi.org/10.1016/S2095-3119\(13\)60702-9](https://doi.org/10.1016/S2095-3119(13)60702-9).

- [29] C. Dong, Z. Zhang, Q. Lu, Y. Yang, Characteristics and mechanism study of analytical fast pyrolysis of poplar wood, *Energy Convers. Manag.* 57 (2012) 49–59. doi:<https://doi.org/10.1016/j.enconman.2011.12.012>.
- [30] R. Widianingsih, H. Hartati, H. Endrawati, J. Mamujaja, Fatty Acid Composition of Marine Microalgae in Indonesia, *J Trop Biol Conserv.* 10 (2013) 75–82.
- [31] Y. Lu, R.B. Levine, P.E. Savage, Fatty Acids for Nutraceuticals and Biofuels from Hydrothermal Carbonization of Microalgae, *Ind. Eng. Chem. Res.* 54 (2015) 4066–4071. doi:10.1021/ie503448u.
- [32] M. Yamada, On the Origin of Aldehydes in Fermentation Products, *Bull. Agric. Chem. Soc. Japan.* 4 (1928) 18–24. doi:10.1080/03758397.1928.10856847.
- [33] K. Pielech-Przybylska, M. Balcerek, A. Nowak, P. Patelski, U. Dziekońska-Kubczak, Influence of yeast on the yield of fermentation and volatile profile of “Węgierka Zwyczajna” plum distillates, *J. Inst. Brew.* 122 (2016) 612–623. doi:10.1002/jib.374.
- [34] A. Kruse, P. Bernolle, N. Dahmen, E. Dinjus, P. Maniam, Hydrothermal gasification of biomass: consecutive reactions to long-living intermediates, *Energy Environ. Sci.* 3 (2010) 136–143. doi:10.1039/B915034J.
- [35] A. Kruse, F. Koch, K. Stelzl, D. Wüst, M. Zeller, Fate of Nitrogen during Hydrothermal Carbonization, *Energy & Fuels.* 30 (2016) 8037–8042. doi:10.1021/acs.energyfuels.6b01312.
- [36] Y. Fan, U. Hornung, N. Dahmen, A. Kruse, Hydrothermal liquefaction of protein-containing biomass: study of model compounds for Maillard reactions, *Biomass Convers. Biorefinery.* (2018). doi:10.1007/s13399-018-0340-8.
- [37] Y. Fan, U. Hornung, N. Dahmen, A. Kruse, 26th European Biomass Conference and Exhibition, 14-17 May 2018, Copenhagen, Denmark, (2018) 14–17.
- [38] C. Falco, M. Sevilla, R.J. White, R. Rothe, M.-M. Titirici, Renewable Nitrogen-Doped Hydrothermal Carbons Derived from Microalgae, *ChemSusChem.* 5 (2012) 1834–1840. doi:10.1002/cssc.201200022.